Proceedings of ASME Turbo Expo 2011
GT2011
June 6-10, 2011, Vancouver, British Columbia, Canada

GT2011-46264

NUMERICAL SIMULATIONS OF TURBULENT MIXING AND AUTOIGNITION OF HYDROGEN FUEL AT REHEAT COMBUSTOR OPERATING CONDITIONS

Elizaveta Ivanova*
Berthold Noll
Peter Griebel
Manfred Aigner

Institute of Combustion Technology
German Aerospace Center (DLR)
Pfaffenwaldring 38-40
70569 Stuttgart
Germany
Email: elizaveta.ivanova@dlr.de

Khawar Syed

ALSTOM Power
Brown Boveri Strasse 7
5400 Baden
Switzerland
Email: khawar.syed@power.alstom.com

ABSTRACT

Turbulent mixing and autoignition of H_2-rich fuels at relevant reheat combustor operating conditions are investigated in the present numerical study. The flow configuration under consideration is a fuel jet perpendicularly injected into a crossflow of hot flue gas ($T > 1000K, p = 15bar$). Based on the results of the experimental study for the same flow configuration and operating conditions two different fuel blends are chosen for the numerical simulations. The first fuel blend is a H_2/natural gas/N_2 mixture at which no autoignition events were observed in the experiments. The second fuel blend is a H_2/N_2 mixture at which autoignition in the mixing section occurred.

First, the non-reacting flow simulations are performed for the H_2/natural gas/N_2 mixture in order to compare the accuracy of different turbulence modeling methods. Here the steady-state Reynolds-averaged Navier- Stokes (RANS) as well as the unsteady scale-adaptive simulation (SAS) turbulence modeling methods are applied. The velocity fields obtained in both simulations are directly validated against experimental data. The SAS method shows better agreement with the experimental results.

In the second part of the present work the autoignition of the H_2/N_2 mixture is numerically studied using the 9-species 21-steps reaction mechanism of O'Conaire et al. [1]. As in the reference experiments, autoignition can be observed in the simulations. Influences of the turbulence modeling as well as of the hot flue gas temperature are investigated. The onset and the propagation of the ignition kernels are studied based on the SAS modeling results. The obtained numerical results are discussed and compared with data from experimental autoignition studies.

NOMENCLATURE

κ	model constant
ρ	density
ω	specific dissipation rate of the turbulent kinetic energy
FI	location of the jet injection point
k	turbulent kinetic energy
L	distance from the jet injection point to the end of the mixing section
p	pressure
$Q_{SST-SAS}$	additional production term in the ω equation of the SST-SAS model
R	ideal gas constant
T	temperature
T_{cf}	temperature value on the inlet of the mixing section

*Address all correspondence to this author.

U_{cf}	absolute mean value of the crossflow velocity
U_j	j component of the flow velocity vector
x, y, z	axes of the Cartesian coordinate system
Y_i	specific mass fraction

INTRODUCTION

The use of H_2-rich fuels in lean premixed combustion systems generally leads to a lower autoignition temperature and flashback margins compared to natural gas [2]. Special challenges arise in the reheat, or sequential, combustion systems such as ALSTOM's $GT24^{®}$ and $GT26^{®}$[1] family [3,4]. This combustion concept is characterized by two fuel injection and energy conversion steps in two separate combustion chambers with an expansion step in a high pressure turbine stage in between. The exhaust gas is then further expanded in a low pressure turbine. The mixing zone of the reheat combustor is characterized by high temperatures (above 1000 K). These conditions lead to extremely short ignition delay times. Knowing the ignition delay times is key for safe GT operation in order to avoid autoignition in the mixing zone.

With the increasing role of simulation in design optimization of GTs the ability of the computational models to predict autoignition phenomena in realistic flow configurations at relevant temperature and pressure conditions becomes very important. Such simulations involve a very complex interplay of turbulence, mixing and chemical reaction models whereas normally the model development and validation is based on academic test cases of simplified subproblems. Detailed studies based on realistic test cases are needed to elucidate the abilities and the limitations of the existing models to predict autoignition under realistic conditions. This forms the focus of the present work.

This study has two main goals. The first one is to perform simulations of the non-reacting test case of the mixing section of a research reheat combustor at relevant temperature and pressure conditions. Here the accuracy of different turbulence modeling concepts for the non-reacting flow field predictions should be compared. The second goal is the simulation of the autoignition and the flame front propagation in the mixing section of the combustor. The achieved results should be compared with the results of the experimental study for the same system. Here a general question about the possibility of the prediction of the autoignition phenomena within the chosen computational framework should be answered. Besides this, studies on the turbulence modeling method dependence as well as on the hot flue gas temperature dependence should be performed. Finally, the results of the unsteady simulations should be analyzed in detail for the description of the autoignition-related flow phenomena which cannot be fully understood based on the experimental results due to measurement technique related limitations.

[1] $GT24^{®}$ and $GT26^{®}$ are registered trademarks of ALSTOM Technology Ltd.

CHOSEN OPERATING CONDITIONS AND COMPUTATIONAL DOMAIN

The computations are performed at the conditions of the research reheat combustor [5, 6] of the Institute of Combustion Technology of the German Aerospace Center (DLR) in Stuttgart. The detailed description of the test rig and of the experimental setup can be found in [5, 6]. For the current simulations the mixing section of this combustor is the object of interest. The mixing section is completely reproduced in the chosen computational domain as shown in Fig. 1.

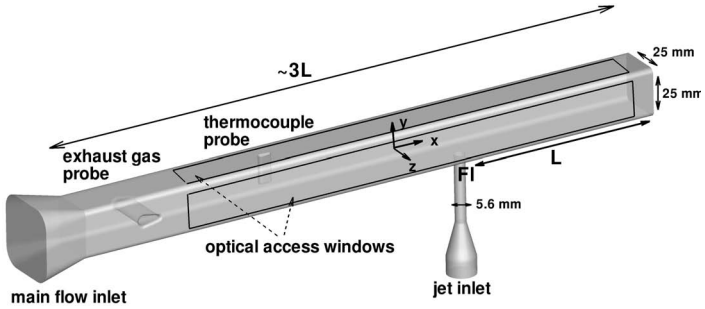

Figure 1. Computational domain.

At the inlet of the mixing section the hot flue gas from the hot gas generator enters a square duct with the cross-section of 25×25 mm. The description of the hot gas generator operating conditions can be found in [5,6]. The temperature (above 1000K) and the O_2 content (about 15 vol.%) of the hot gas are typical for reheat combustors. The total hot gas mass flow rates on the mixing section inlet are between 260-550 g/s which leads to velocities of above 150 m/s. In the calculations the constant mass flow rate identical to the experimental values was set at the mixing section inlet (with a constant velocity distribution over the inlet cross-section). The temperatures at the inlet of the mixing section were set in the non-reacting flow simulations to a constant value corresponding to the experimental conditions. The pressure in the mixing section is 15 bar.

The main channel of the mixing section includes an exhaust hot gas emission probe and a thermocouple probe located upstream of the fuel injection. Both geometries are reproduced in the computational domain (figure 1).

The fuel is injected from the lower wall of the mixing section in a jet in crossflow configuration as shown in figure 1. The diameter of the fuel injector is 5.6 mm. A carrier medium (nitrogen) is injected together with the fuel in order to achieve the

desired jet to crossflow momentum flux ratio and hence the desired penetration depth. The carrier to fuel mass flow ratios are equal to 1 in the considered test cases. The fuel/carrier temperature is 313K. Based on the results of the experimental study [5] two different fuel blends are chosen for the numerical simulations. The first fuel blend is a H_2/natural gas/N_2 (76/4/20 vol.%) mixture at which no autoignition events were observed in the experiments. The jet to crossflow momentum ratio for this fuel blend is 1.7. The second fuel blend is a H_2/N_2 mixture at which ignition in the mixing section was observed. The hydrogen fuel concentration of this mixture at which autoignition occurred in the experiments [5] was 50 vol.%.

In the experiments the optically accessible mixing section parts were convectively air-cooled and the metal parts were water-cooled. The heat losses in the mixing section were estimated to be about 6% in the experiments [5]. The heat losses were taken into account in the simulation by the application of the negative heat fluxes in the respective cooled zones according to the experimental estimation.

COMPUTATIONAL APPROACHES

Turbulence Modeling

In the present work two different turbulence modeling approaches are applied: steady-state Reynolds-Averaged Navier-Stokes (RANS) and unsteady Scale-Adaptive Simulations (SAS) [7]. For the RANS simulations the shear-stress transport (SST) $k-\omega$ turbulence model in its later formulation [8] is applied. Additionally, the universal wall functions approach according to [9] is used. This approach extends the standard turbulent wall boundary condition of the SST $k-\omega$ model in order to avoid a non-physical solution in the regions where the grid could not be sufficiently refined. All the model constants and limiters are as described in [8]. For the Scale-Adaptive Simulations the SST-SAS model is used [7]. The idea behind this model is an additional production term $Q_{SST-SAS}$ in the ω equation of the SST $k-\omega$ model:

$$Q_{SST-SAS} = max\left[\widehat{\zeta}\kappa S^2\frac{L_t}{L_{vK}} - C\cdot\frac{2}{\sigma_\phi}k \cdot max\left(\frac{1}{\omega^2}\frac{\partial\omega}{\partial x_j}\frac{\partial\omega}{\partial x_j}, \frac{1}{k^2}\frac{\partial k}{\partial x_j}\frac{\partial k}{\partial x_j}\right), 0\right]. \quad (1)$$

Here $\widehat{\zeta} = 3.51$, $C = 2$, $\kappa = 0.41$, $\sigma_\phi = 2/3$ are the model constants. The SAS term comes into effect when the ratio of the turbulent length scale, $L_t = k^{1/2}/\omega$, to the von Karman length scale, L_{vK}, increases. The von Karman length scale is based on the ratio of the first to the second velocity derivative (see [7,8,10] for details). L_{vK} is smaller for an unsteady velocity profile than for a steady velocity profile. When the grid is fine enough and the flow equations are able to resolve the small-scale movements, the SAS term detects the unsteadiness and increases the production of the dissipation rate ω. The result is that the turbulent viscosity ν_t is reduced. Thereby the dissipating (damping) effect of the turbulent viscosity on the resolved fluctuations is reduced. Then the momentum equations work in a "LES - like" mode. Further details concerning the SST-SAS model can be found in [7, 8] and examples of its application for simulations of flow patterns similar to considered here in [11, 12].

Mixing Modeling in the Non-Reacting Flow Simulations

In the non-reacting flow simulations both the jet and the crossflow were considered as ideal gases with two different ideal gas constants calculated based on the experimentally determined gas composition. Density calculations of the jet and the crossflow gas mixture were based on the ideal gas equation:

$$\rho_{mix} = \left(\sum\frac{Y_i}{\rho_i}\right)^{-1}, \quad (2)$$

with

$$\rho_i = \frac{p}{R_i T}. \quad (3)$$

The transport equation for the jet gas mass-fraction as well as the energy equation in the temperature form were solved and closed using the gradient diffusion hypothesis with the constant values of the turbulent Prandtl/Schmidt numbers equal to 1. Previous studies [12] have shown that the turbulent Prandtl/Schmidt number values have no significant influence on the mixing predictions in the LES-like mode regions of the SAS simulations.

Combustion Modeling

For the combustion modeling in the reacting case simulations the finite-rate combustion model was used in combination with the assumed joint PDF approach. A detailed description of the used combustion modeling technique can be found in [13].

The employed reaction mechanism is the 9-species 21-steps scheme of O'Conaire et al. [1]. It has been validated against experimental data in the ranges of $0.05-87$ bar pressure, $298-2700$ K temperature and $0.2-6.0$ equivalence ratio. This mechanism is widely accepted for the combustion simulations at a large range of temperatures and pressures.

Numerical Scheme

All models considered here were implemented in the DLR combustion CFD research code THETA. The THETA code flow

solver works on 3D unstructured grids and is designed for the calculations of low Mach number flows with strongly varying density/temperature fields. As recommended in [7] for the SST-SAS model a calibration procedure using the decaying isotropic turbulence test case was applied in order to obtain the calibration constant of the lower limiter of L_{vK} corresponding to the THETA code flow solver. The details of this procedure are described in [7]. For the THETA code flow solver the value of the calibration constant is $C_s = 0.145$.

In the steady-state RANS simulations for the spatial discretization of the convective terms of all transport equations the second order linear-upwind discretization scheme is used. In the SAS calculations for the spatial discretization of the convective terms of the momentum equations the second order central differencing scheme was used, for the spatial discretization of the convective terms of all other transport equations the the second order linear-upwind discretization scheme was used. For the pressure-velocity coupling in the steady - state RANS simulations, the SIMPLE method [14] was used. In the unsteady SAS simulations, a projection method [15] was used. For the time discretization the second order Backward Differentiation Formula (BDF) [16] was used.

Computational Grids and Time Stepping

All calculations were performed on polyhedral unstructured grids with hexahedra-layers on the walls (figure 2). The grid in the steady-state RANS computations had around 650 000 points whereas the SAS computations were performed on grids containing around 950 000 points. The grids are refined in the important flow regions (jet shear layers) based on the results of preliminary calculations using the grid adaptation procedure available in the DLR THETA code. An example of such a grid used for the SAS simulations can be seen in figure 2.

The time step in the SAS calculations was about 10^{-7}s, which leads to maximal Courant-Friedrichs-Lewy numbers of 2. All time-averaged results presented below are obtained after about 5 residence times ($5L/U_{cf}$).

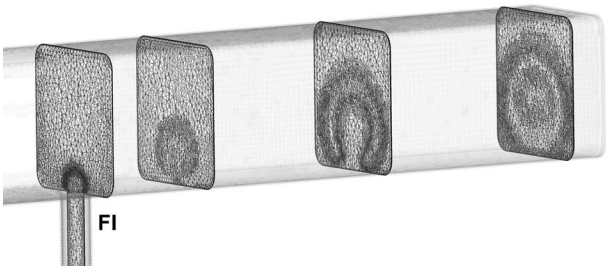

Figure 2. Computational grid for the SAS simulations. Cross-sections in different positions along the mixing zone of the main channel.

RESULTS AND DISCUSSION

Non-Reacting Flow Simulations

First the turbulent mixing simulations of the non-reacting H_2/natural gas/N_2 fuel blend in the hot flue gas are performed. The resulting (time-averaged for SAS) velocity field predictions are compared with the results of the PIV measurements performed in the respective experimental study [5]. The distributions of the x- and the y- components of the velocity vector are shown in figures 3 and 4. The SAS results show better agreement with the experimental data than the RANS results. It can be seen in figure 3 that the recirculation zone after the jet injection location is strongly overpredicted by RANS whereas SAS simulations are more accurate regarding the recirculation zone position and strength. Consequently RANS also strongly overestimates the vertical velocity in the region near to the lower channel wall (figure 4(b)) which is not the case in the SAS simulation (figure 4(c)). A lack of accuracy in the RANS velocity field and mixing predictions for a jet in crossflow configuration was already observed by the authors of the current paper in the earlier publications [11, 12].

Both RANS and SAS slightly overestimate the vertical velocity U_y in the jet core (figure 4). However here again RANS shows more discrepancy with experimental data. The same

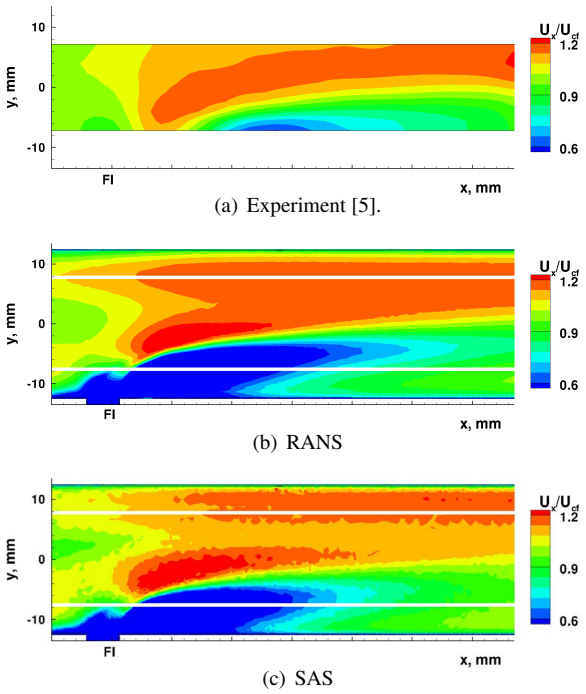

(a) Experiment [5].

(b) RANS

(c) SAS

Figure 3. Distribution of the (time-averaged) x-component of the velocity vector U_x non-dimensionalized by the mean crossflow velocity U_{cf}. Horizontal white lines in the plots of the simulation results mark the edges of the optical access in the experiments [5].

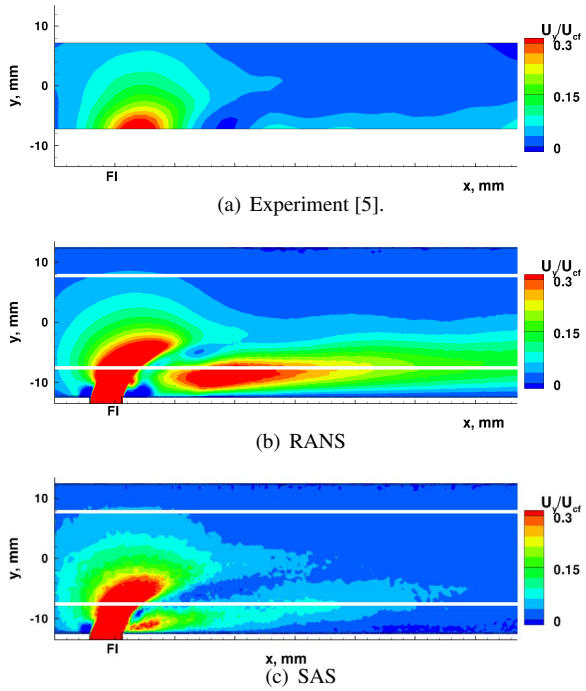

Figure 4. Distribution of the (time-averaged) y-component of the velocity vector U_y non-dimensionalized by the mean crossflow velocity U_{cf}. Horizontal white lines in the plots of the simulation results mark the edges of the optical access window of experiments [5].

trends for both RANS and SAS were previously reported in [12].

Autoignition Simulations

In the second part of this work the autoignition simulations were performed for the case of the H_2/N_2 fuel blend injection. The baseline turbulence modeling technique applied here is the SAS. In all unsteady autoignition simulations first the pure N_2 jet was injected into a crossflow with the desired mass flow ratio. After the establishing of the fully developed flow field under the given conditions the pure N_2 was exchanged by the carrier N_2 and H_2/N_2 50/50 vol. mixture. From that moment on the data "snapshots" were taken in order to observe the autoignition phenomena. Such a procedure is similar to the time-ramping of the H_2 mass flow rate which was applied in the autoignition experiments of [5,6].

In the present study isosurfaces of the OH mass fraction Y_{OH} were chosen to be the flame front indicator. The isosurface of $Y_{OH} = 0.0001$ at different time points of the SAS simulation is presented in figure 5. The data snapshot in figure 5(a) was taken shortly after the first occurrence of the ignition kernels. This time point is chosen to be a reference time point. The ignition first occurs at the beginning of the second third of the distance L between the jet injection location and the end of the mixing section. Similar axial positions of the ignition kernels were reported in the experimental study of Fleck at al. [5].

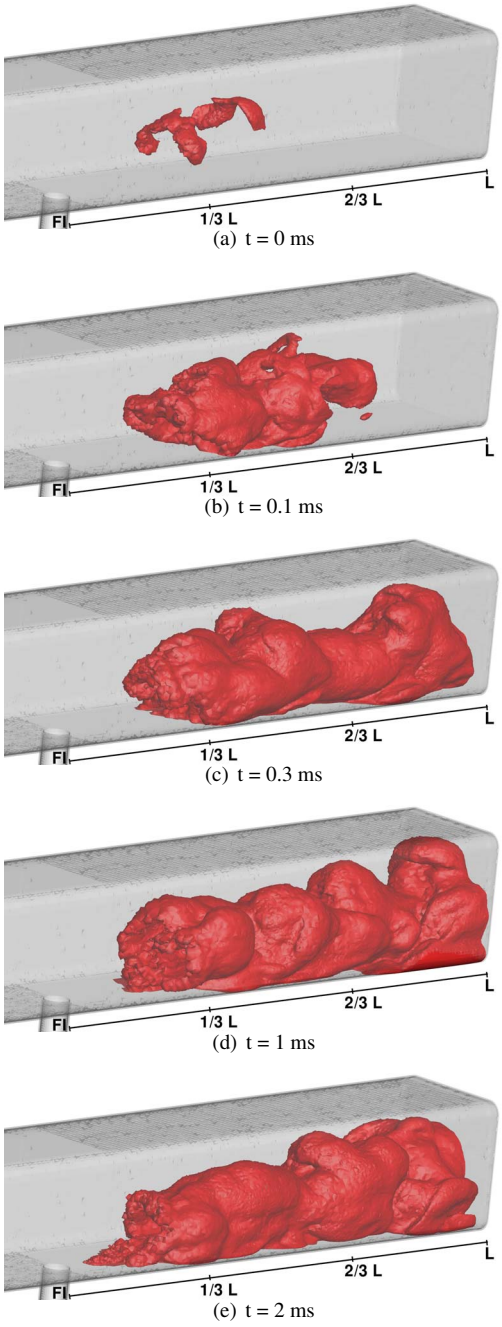

Figure 5. Isosurfaces of $Y_{OH} = 0.0001$ at different time points of the SAS simulation.

Then the flame starts to propagate downstream along the jet shear layer as seen in figure 5(b). In the moment t = 0.1 ms the flame is located almost entirely between $1/3L$ and $2/3L$. The same situation was observed in the experiments [5] at the same

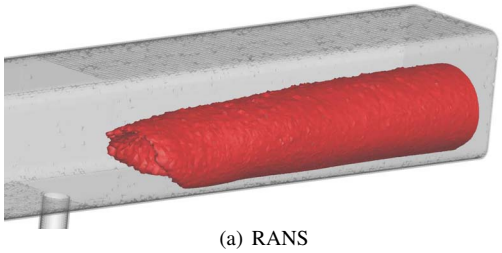

(a) RANS

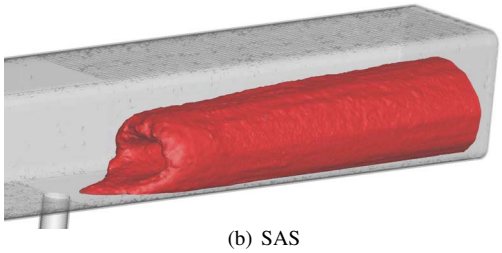

(b) SAS

Figure 6. Stable flame isosurfaces of $Y_{OH} = 0.0001$.

time point.

Not only the downstream but also the upstream flame propagation is typical for this flow pattern. This fact becomes especially evident at a later point in time between 1 and 2 ms (figures 5(d) and 5(e)). Here the flame propagation upstream of the initial ignition location can be observed especially near to the lower wall of the mixing section. This behavior has also been observed in the experiments [5]. However in the experiments this phenomenon could not be described in detail because of the limited optical access in the boundary layer region. The present simulation reveals the upstream transport of the flame in the boundary layer visible by the flame beeing attached to the wall. The reasons for the upstream near-wall flame propagation are not clear at present but should be clarified in the future. A possible explanation can be the transport of the flame along the complex vortical structures formed in the jet in crossflow configuration [17] and their interaction with the wall boundary layer. A more detailed study of the flame-vortex interaction is needed.

Thus the flame propagation processes can be described fairly well by SAS. In contrast to SAS, RANS as a steady-state approach is able to represent only the stable time-averaged flame front which establishes after ignition. The comparison of this RANS solution with the time-averaged SAS results (averaging over the time range 2-8 ms) is presented in figure 6. The form of the $Y_{OH} = 0.0001$ isosurfaces near the lower wall of the mixing section is different. In RANS the near-wall flame is absent in the first third of the mixing section (figure 6(a)). However the indications of the flame presence in this region in the stabilized combustion phase have been reported in the experimental investigations [5] and the flame is clearly seen in the time-averaged SAS results (figure 6(b)). A better ability of the SAS to predict the near-wall upstream flame propagation can be explained by

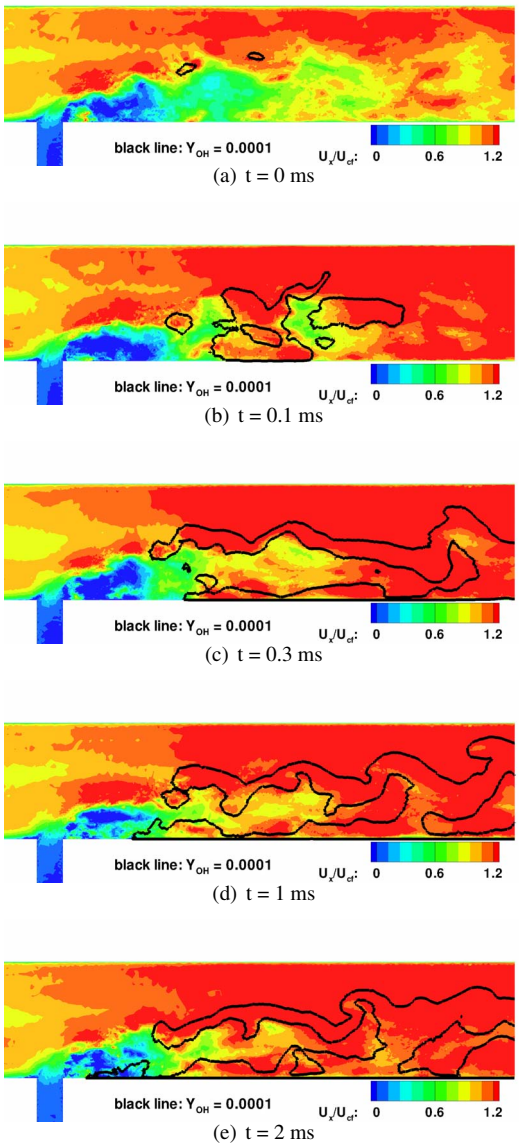

Figure 7. Distribution of the x-component of the velocity vector U_x non-dimensionalized by the mean crossflow velocity U_{cf}. The isolines of $Y_{OH} = 0.0001$ are shown to indicate the flame front position.

the good resolution of the jet in crossflow vortical structures in such simulations [11].

Additional analysis of the flow and the temperature field during the autoignition process can be performed based on the SAS simulation results. An example of such an analysis is given in figures 7, 8, 9. In figure 7 the instantaneous U_x velocity field is presented. It can be seen that after the autoignition took place the absolute velocity downstream of the ignition location increases. The velocity field near the jet injection seems to be only slightly

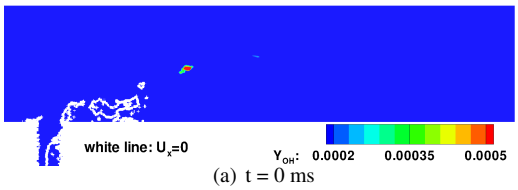

(a) t = 0 ms

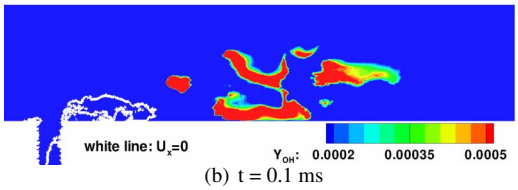

(b) t = 0.1 ms

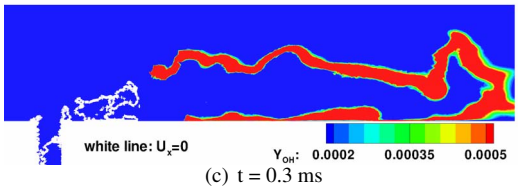

(c) t = 0.3 ms

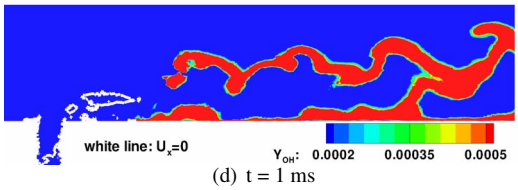

(d) t = 1 ms

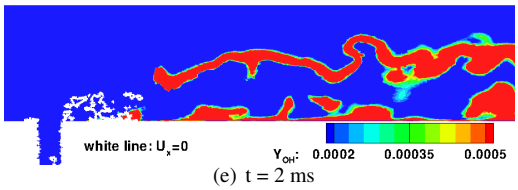

(e) t = 2 ms

Figure 8. Distribution of the Y_{OH} contours. The isolines of $U_x = 0$ are shown to indicate the recirculation zone position.

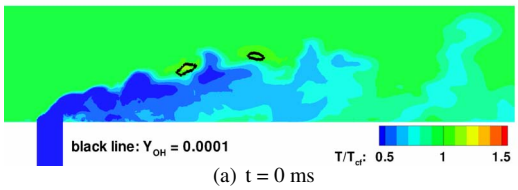

(a) t = 0 ms

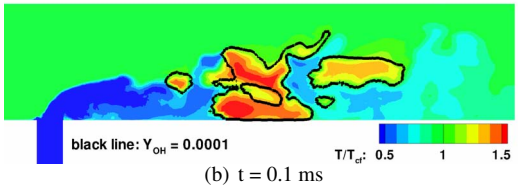

(b) t = 0.1 ms

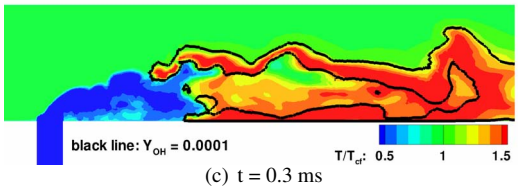

(c) t = 0.3 ms

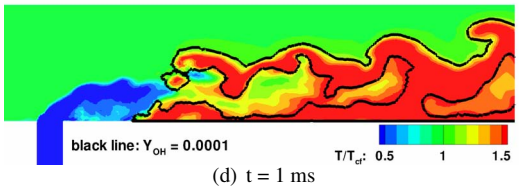

(d) t = 1 ms

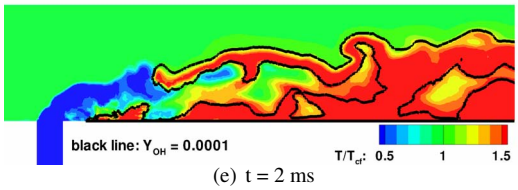

(e) t = 2 ms

Figure 9. Distribution of flow temperature T non-dimensionalized by the crossflow inlet temperature T_{cf}. The isolines of $Y_{OH} = 0.0001$ are shown to indicate the flame front position.

influenced by the ignition. Figures 7 and 8 also reveal that the upstream flame propagation near to the lower wall is not the result of the recirculation zone behind the jet. Figure 8 clearly shows that the regions of the negative x-velocities are very small and occur only near to the jet injection location. The flame propagates upstream without being in the recirculation zone. This is an additional indication for the assumption given above that the upstream flame propagation occurs due to a more complex flame-vortex interaction.

Figure 9 shows the dimensionless temperature field obtained in the presented simulations. It can be seen that the regions of the high temperatures correlate very well with the $Y_{OH} = 0.0001$ isolines. It can be also seen that the regions of the high temperature correlate with the shear layer zones and in the jet core region the flow remains relatively cold.

It should be mentioned here that the hot flue gas temperature in the main inlet of the mixing section was about 120K ($\sim 10\%$) higher than in the respective experimental measurements [5]. The position and the general occurrence of the flame

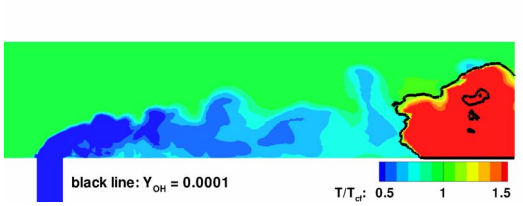

Figure 10. Distribution of flow temperature T non-dimensionalized by the crossflow inlet temperature T_{cf}. T_{cf} is 60K lower than in the basic case. t = 2 ms. The isolines of $Y_{OH} = 0.0001$ are shown to indicate the flame front position.

in the simulation were very sensitive to the temperature conditions of the hot flue gas. This can be seen in figure10. This figure shows the flame position obtained in the simulation with the flue gas inlet temperature 60K below the basic simulation case (60K above the experimental flue gas inlet temperature) at the time point of t = 2 ms after the first occurrence of the ignition kernel. It is seen that the flame is located in the last third of the mixing section. The further decreasing of the flue gas inlet temperature down to experimental values leads to the absence of the autoignition in the simulation. In the experiments [5, 6] also an observation was made that the autoignition and the flame propagation are very sensitive to the hot flue gas temperature. The general discrepancy between the experimental and the simulated autoignition temperatures can be explained by the deficits of the chemical reaction mechanism. Here a detailed chemical reaction mechanism study in the present flow conditions is needed to clarify the sensitivity of the simulated autoignition and the flame propagation on the chemistry modeling.

SUMMARY AND CONCLUSIONS

Turbulent flow field, autoignition, and flame propagation in the mixing section of a research reheat combustor are simulated successfully in the present work. The results obtained using both the steady-state RANS and the unsteady vortex-resolving SAS turbulence modeling methods are presented.

The cold flow simulations show that SAS method represents the experimental velocity field better than RANS. It should however be mentioned that the computational cost which was needed to obtain a time-averaged SAS solution in the current calculations was about 50 times higher than the computational cost of RANS simulations. Thus in practical applications the decisions about suitability of different turbulence modeling methods should be made depending on the aims of each calculation and availability of the computational resources.

One application field where the unsteady vortex-resolving methods are unavoidable are the detailed temporal studies of the autoignition phenomena such as one presented in the second part of this work. In contrast to RANS, SAS is able to represent the autoignition and flame propagation processes in detail as a function of time. Comparison of the obtained results with experimental observations made in [5] also allow the statement that SAS simulation represents the real flame propagation processes fairly well. This makes SAS simulations very useful to complement the results of the experimental studies. In such a "numerical experiment", the autoignition-related phenomena can be studied in the zones which are optically not accessible in the measurements. In the present work it was the boundary-layer zone of the mixing section. The simulation reveals that this zone plays an important role in the upstream flame propagation.

Furthermore, from a simulation a variety of flow parameters can be extracted and analyzed which are difficult to measure in the entire flow field at the same time (local pressures, temperatures, velocities, species concentrations etc.). Thereby numerical simulations help to gain a better understanding of the autoignition and the flame propagation processes.

Thus, a general conclusion can be drawn that the autoignition phenomena in reheat combustion applications can be successfully simulated by the high-end CFD and combustion modeling methods. Further development and testing of those methods can promise an increasing role of the numerical simulations in the detailed understanding of the physical processes in the considered configurations.

ACKNOWLEDGMENT

The authors are grateful to the ALSTOM Power Generation AG for the encouragement of the present study. We also would like to thank Julia Fleck, Michael Stöhr and Rajesh Sadanandan (Institute of Combustion Technology, DLR) for their support and discussions regarding the experimental data, Guido Schmitz (Institute of Combustion Technology, DLR) for his help in generating the grids, and Massimiliano Di Domenico (Institute of Combustion Technology, DLR) for his kind THETA code support. The Jülich Supercomputing Center is acknowledged for the computational time provided under the NIC project number 3793.

REFERENCES

[1] O'Conaire, M., Curran, H., Simmie, J., Pitz, R., and Westbrook, C., 2004. "A comprehensive modeling study of hydrogen oxidation". *International Journal of Chemical Kinetics*(11), pp. 602–622.

[2] Lieuwen, T., McDonnel, V., Petersen, E., and Santavicca, D., 2008. "Fuel flexibility influences on premixed combustor blowout, flashback, autoignition and stability". *J. Eng. Gas Turbines Power*(130), pp. 011506 1–10.

[3] Joos, F., Brunner, P., Schulte-Werning, B., Syed, K., and Eroglu, A., 1996. "Development of the sequential combus-

tion system for the ABB GT24/GT26 gas turbine family". ASME Paper 1996-GT-315.

[4] Güthe, F., Hellat, J., and Flohr, P., 2009. "The reheat concept: the proven pathway to ultralow emissions and high efficiency and flexibility". *J. Eng. Gas Turbines Power*(131), pp. 021503 1–7.

[5] Fleck, J. M., Griebel, P., Steinberg, A. M., Stöhr, M., and Aigner, M., 2010. "Experimental investigation of a generic, fuel flexible reheat combustor of a gas turbine relevant operating conditions". In Proc. ASME Turbo Expo 2010: Power for Land, Sea and Air, Glasgow, UK. GT2010-22722.

[6] Fleck, J., Griebel, P., Steinberg, A. M., Stöhr, M., Aigner, M., and Ciani, A., 2011. "Autoignition limits of hydrogen at relevant reheat combustor operating conditions". In Proc. ASME Turbo Expo 2011: Power for Land, Sea and Air, Vancouver, Canada. GT2011-46195.

[7] Egorov, Y., and Menter, F., 2008. "Development and application of SST-SAS turbulence model in the DESIDER project". In *Adwances in Hybrid RANS-LES Modelling*, S.-H. Peng and W. Haase, eds. Springer Verlag Beriln Heidelberg, pp. 261–270.

[8] Menter, F. R., 2009. "Review of the shear-stress transport turbulence model experience from an industrial perspective". *International Journal of Computational Fluid Dynamics,* **23**(4), pp. 305–316.

[9] Esch, T., and Menter, F. R., 2003. "Heat tranfer prediction based on two-equation turbulence models with advanced wall treatment". In Turbulence, Heat an Mass Transfer 4, K. Hanjalic, Y. Nagano, and M. Tummers, eds.

[10] Menter, F. R., and Egorov, Y., 2005. "A scale-adaptive simulation model using two-equation models". AIAA Paper 2005-1095.

[11] Ivanova, E., Noll, B., Di Domenico, M., and Aigner, M., 2009. "Unsteady simulations of flow field and scalar mixing in transverse jets". In Proc. ASME Turbo Expo 2009: Power for Land, Sea and Air, Orlando, Florida, USA. GT2009-59147.

[12] Ivanova, E., Noll, B., and Aigner, M., 2010. "Computational modelling of turbulent mixing of a transverse jet". In Proc. ASME Turbo Expo 2010: Power for Land, Sea and Air, Glasgow, UK. GT2010-22764.

[13] Di Domenico, M., Kutne, P., Naumann, C., Herzler, J., Sadanandan, R., Stoehr, M., Noll, B., and Aigner, M., 2009. "Numerical and experimental investigation of a semi-technical scale burner employing model syntetic fuels". In Proc. ASME Turbo Expo 2009: Power for Land, Sea and Air, Orlando, Florida, USA. GT2009-59308.

[14] Patankar, S. V., 1980. *Numerical heat transfer and fluid flow*. Series in Computational Methods in Mechanics and Thermal Science. Hemisphere Publishing Corporation.

[15] Chorin, A., 1968. "Numerical solution of Navier-Stokes equations". *Mathematics of Computation,* **22**(104), p. 745.

[16] Gerlinger, P., 2005. *Numerische Verbrennungssimulation (Numerical combustion simulation)*. Springer, Berlin Heidelberg. In German.

[17] Fric, T., and Roshko, A., 1994. "Vortical structure in the wake of a transverse jet". *J. Fluid Mech.,* **279**, pp. 1–47.

